J Polym Res (2013) 20:178
DOI 10.1007/s10965-013-0178-5

ORIGINAL PAPER

Behavior of epoxy composite resins in environments at high moisture content

Luigi Vertuccio · Andrea Sorrentino · Liberata Guadagno · Valeria Bugatti · Marialuigia Raimondo · Carlo Naddeo · Vittoria Vittoria

Received: 21 December 2012 / Accepted: 15 May 2013 / Published online: 28 May 2013

Abstract Three different organo-modified clays have been incorporated by sonication into a high performance epoxy resin before the cross-linking reaction. The X-ray analysis indicated that, depending on the organoclay type, partially exfoliated and partially intercalated composites have been obtained. As shown by the DSC analysis, the clay addition seems to interact with the cross-linking reaction. The incorporation of organoclay into epoxy increased free volume and micro-voids in the samples. Sorption of water in the composite samples resulted higher than that of the pristine resin, whereas the diffusion coefficient is significantly lower. The lower value of diffusion makes the permeability at ambient conditions lower than the pristine resin. The elastic modulus of the composite sample results higher than that of the pristine resin, especially in the temperature region around the glass transition. The presence of organoclay in epoxy matrix decreased the glass transition temperature, whether the nanocomposites were in a dry or wet condition.

Keywords Epoxy resin composites · Cationic clays · Cure behaviour · Mechanical properties · Thermal properties

Introduction

Epoxy resins are widely used as matrices for structural composite materials, adhesives, and organic coatings due to their good mechanical and insulating properties [1, 2]. However, it is well known that these good properties are strongly affected by water in the environment. Indeed water in the polymer acts as a plasticizer diminishing the mechanical properties and damaging the chemical structure of the matrix for hydrolysis reactions [3]. This effect is a heavy drawback in aeronautical applications, since aircrafts are exposed to very humid and rainy environments.

Water transport is related to the availability of molecular-sized holes in the polymer structure and to the polymer–water affinity. The availability of holes depends on the polymer structure, morphology, filler and crosslink density. The polymer–water affinity is related to the presence of hydrogen bonding sites along the polymer chains, which create attractive forces between the polymer and the water molecules [4, 5].

The nature of epoxy–water molecule interactions has been investigated by using various techniques. Apicella et al. [6, 7] proposed three different modes for the water sorption of epoxy systems: (a) bulk dissolution of water in the polymer network; (b) moisture sorption onto the surface of holes that define the excess free volume of the glassy structure; and (c) hydrogen bonding between hydrophilic groups of the polymer and water. Moy and Karasz [8], Mikols et al. [9], and Pethrick et al. [10] reported that, in epoxy compounds, water exists in two distinct forms: free water that fills the microcavities of the network and bound water in strong interactions with polar segments. Two possible mechanisms have been suggested for the explanation of the degradation occurring in most composite systems: matrix plasticization and degradation due to hydrolytic reactions.

Water absorbed by epoxy matrix composites plays the role of plasticizer, as evidenced by the reduction in the matrix glass transition temperature, Tg [11, 12]. This effect is usually reversible when water is removed, showing that water can fill the free volume and can be removed without changing the properties. At variance exposure to water at elevated temperatures, or the presence of water strictly bound with hydrogen bonds to the polymeric chains can produce, for long times,

L. Vertuccio (✉) · L. Guadagno · V. Bugatti · M. Raimondo · C. Naddeo · V. Vittoria
Dipartimento di Ingegneria Industriale, Università di Salerno,
Via Ponte Don Melillo,
84084 Fisciano, SA, Italy
e-mail: lvertuccio@unisa.it

A. Sorrentino
CNR, Institute for Composite and Biomedical Materials (IMCB),
Piazzale Enrico Fermi 1,
80055 Portici, NA, Italy

irreversible effects, which can be attributed to chemical degradation of the matrix through hydrolytic reactions, as well as expansion and microcracking of internal voids.

Currently both chemical and physical modifications of epoxy systems are being deeply investigated to reduce water permeability [13–16]. Among the physical modifications, polymer–clay composites have attracted considerable attention for improving the polymer properties. In particular, nanostructured modification of polymers, using inorganic fillers dispersed at nanoscale, has opened up new perspectives for multi-functional materials. By choosing the appropriate filler, unprecedented morphological control down to the nanoscale is obtained [17–19]. The potential for these new multifunctional materials lies in the simplicity with which this filler can be added to the polymer matrix [20]. Tailoring of the polymer-filler interface is of key importance, since the structures generated at the nanoscale are the result of a fine balance of competing interactions, and those at the inter phases are indeed the most important ones [15]. With emerging availability of nanometer feature materials such as clays, carbon nanotubes, fibers, plates, and particles, coupled to a growing ability to characterize and manipulate systems at this scale, nano-engineered multifunctional materials could hold the key to future development and use of superperforming composites for several advanced applications [17, 21, 22]. The challenge is to obtain the best dispersion of the inorganic filler, so using small filler quantities. In the case of clay the challenge is to exfoliate the clay into the polymer, so reinforcing the matrix and making very tortuous the water molecule path. In this paper the effect of the addition of different cationic organo-clays to an epoxy resin to be used for structural aeronautical applications was investigated. In particular, the barrier to the water permeability was characterized with the aim to correlate the resulting properties to the clay type, concentration and dispersion.

Experimental

The epoxy resins diglycidyl ether of bisphenol A (DGEBA) and the hardener 4,4 diaminodiphenylsulfone (DDS) were supplied by Aldrich Chemicals. The organoclays were supplied by Süd-Chemie and Southerm Clay for Nanofil 804 and Cloisite 93A and Cloisite 30B respectively. Epoxy resin and the hardner DDS were mixed at 120 °C and the clay powder was added and dispersed with high power ultrasonic probe. The mixture was cured at 150 °C for 1 h followed by 3 h at (220 °C). The organoclay content in the samples was controlled by thermogravimetric analysis.

The samples are coded as EDSXClay, where X represents the organoclay concentration (for example EDS3C30B means a concentration of Cloisite 30B of 3 %). The information about the type of the surfactants used for organophilization is summarized in Table 1.

Methods

X-ray diffraction (XRD) measurements were performed with a Brucker D8 Advance diffractometer with Ni-filtered CuKa radiation (k=1.54184A°).

Thermogravimetric Analysis (TGA) was carried out from 25 °C to 900 °C (heating rate of 10 °C/min) under air flow, using a Mettler TGA/SDTA 851.

The transmission electron microscopy (TEM) characterization was performed on a JEOL 2010 LaB6 microscope operating at 200 kV. TEM samples were cut from nanocomposite blocks using an ultramicrotome equipped with a diamond knife at ambient temperature.

Thermal analysis (DSC) was performed with a differential scanning calorimeter Mettler DSC 822 in a flowing nitrogen atmosphere. The curing reaction of the resins with and without organoclay was performed in dynamic regime, by heating in the Differential Scanning Calorimeter at 10 °C/min from −60 °C to 400 °C.

Density of the composite samples were measured by a flotation method using mixtures of liquids with a higher and lower density, that is chloroform (d=1.481 g/cm^3) and n-hexane (d=0.656 g/cm^3) respectively. All the specimens were dried in an oven at 50 °C and allowed to cool to room temperature in a desiccator. After immersion, the specimens were taken out from the mixture and dried with a clean dry cloth. The specimens were reweighed to the nearest 0.1 mg in order to exclude any possible absorption of liquid into the samples.

Transport properties were performed using a sensitive helical spring suspended in an all-glass thermoregulate chamber. The spring extension with load is accurately calibrated using platinum weights at the temperature of the experiments. The recorded weight is corrected for buoyancy to obtain the mass of the sample.

Dynamic mechanical properties of the samples were determined with a dynamic mechanical thermo-analyzer (TA instrument-DMA 2980). Solid samples with dimensions 4×10×35 mm were tested by applying a variable flexural deformation. The displacement amplitude was set to 0.1 %, whereas the measurements were performed at the frequency of 1 Hz. The range of temperature was from −60 °C to 300 °C at the scanning rate of 3 °C/min.

Results and discussion

X-ray analysis

In Fig. 1 the X-ray diffractograms of the epoxy matrix (Fig. 1a) and the composites cured in the presence of 3 % of various organoclays (Fig. 1b, c, d) are reported. For comparison the diffractograms of the pristine organoclay are shown, too.

Table 1 Characteristics of the investigated layered silicates

Clay	Surfactant chemical Name	Density [g/cm^3]	Surfactant chemical structure
Nanofil 804®	Stearyldihidroxyethylammonium chloride	1,8	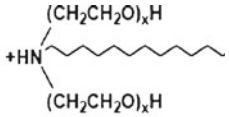
Cloisite 93A®	Methyl Hydrogenated Tallow Ammonium	1,88	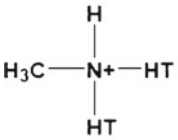
Cloisite 30B®	Methyl Tallow Bis-2-Hydroxyethyl Ammonium	1,98	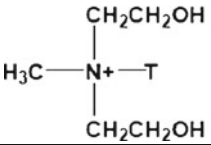

Tallow = T = Chaine alkyle = 65 % $C_{18}H_{37}$, 30 % $C_{16}H_{33}$, 5 % $C_{14}H_{29}$

In the diffractogram of sample EDS3N804 (Fig. 1b), the basal spacing peak of the pristine organoclay almost disappeared, indicating that the clay sheets were exfoliated during the curing reaction. At variance in the diffractogram of sample EDS3C93A (Fig. 1c) an intense peak at 2.35° of 2ϑ (d-spacing=3.76 nm) is present. If compared with the basal peak in the pristine organoclay, appearing at 3.6° of 2ϑ (d-spacing=2.45 nm), it is possible to deduce that the clay sheets were enlarged and therefore the resin was partially intercalated into the clay sheets. For sample EDS3C30B (Fig. 1d) the basal peak of the organoclay (4.95° of 2ϑ) is absent and only a shoulder at lower angle (2.45° of 2ϑ) is apparent. This result indicates an almost complete exfoliation with a small fraction of an intercalated structure. To

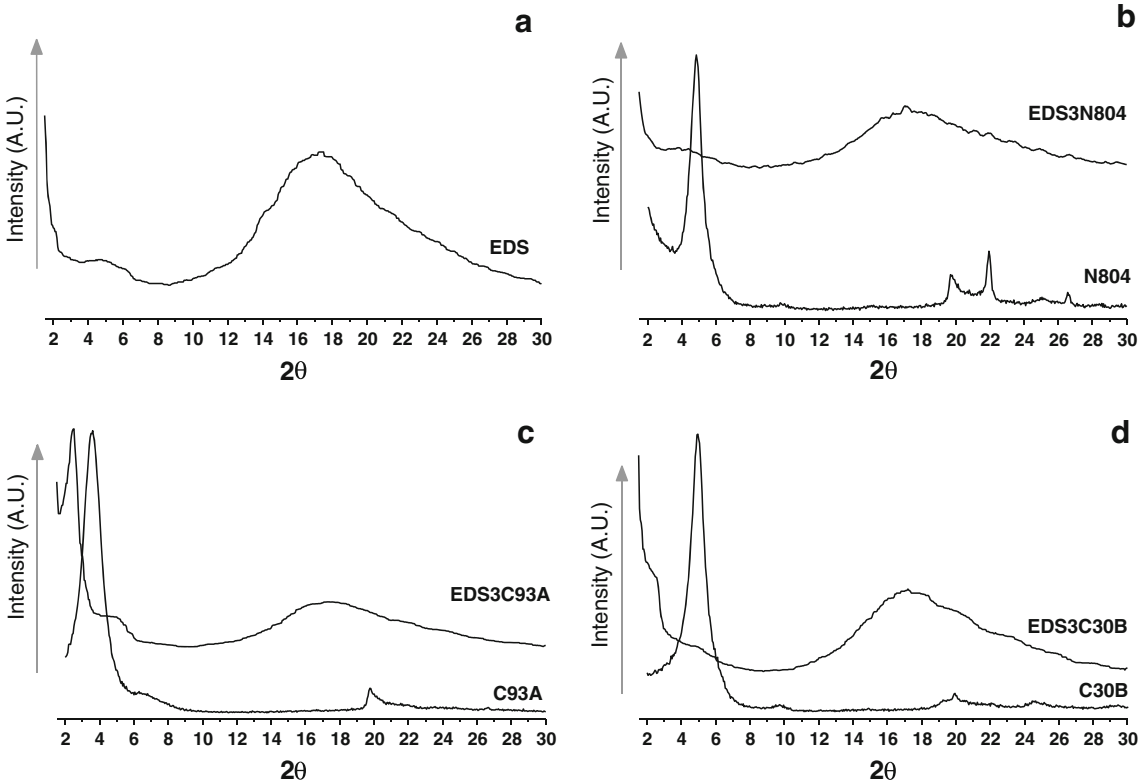

Fig. 1 X-ray diffractograms of the different samples: **a** epoxy matrix; **b** Nanofil 804 with the relative 3 % composite; **c** Cloisite 93A with the relative 3 % composite; **d** Cloisite 30B with the relative 3 % composite

investigate the influence of the organoclay concentration on the possibility to obtain the exfoliation, samples with different concentrations of Cloisite 30B were prepared. In Fig. 2 are reported the X-ray diffratograms of these composites.

Both the samples with 5 % and 7 % show the peak of the pristine organoclay, although of reduced intensity, and a peak at about 2.45° of 2θ, indicating a partial intercalation of the resin into the clay lamellae. These results indicate that, in our experimental conditions, the exfoliation of the clay C30B can occur up to a concentration of 3 %, whereas at higher concentrations the sample cannot be considered free from big clay tactoids.

Morphological analysis

TEM images at both low and high magnifications are shown for sample EDS3C30B in Fig. 3. The clay presents dimensional size one micron in length and thickness in a range from 400 to 500 nm (TEM image not reported here). The thickness of the clay packet is reduced up to values between 80 and 50 nm (Fig. 3b, c) with an estimated d-spacing of 7–15 nm. In Fig. 3, the dark lines are the silicate layers of nanoclay and the white area in the vicinity of the clay layers is formed due to cutting. Figure 3 shows that the agglomerates of nanoclay were broken down to form small particles consisting of several clay platelets. Probably the morphology of the resultant nanocomposites is a combination of both exfoliation and disordered intercalation that explains the observed absence of peak in the XRD diagrams. A similar result was obtained using the same clay from Yasmin et al. [23]. The exfoliated morphology is clear from micrograph (Fig. 3b, c) where each layer of nanoclay is randomly distributed in epoxy matrix. It is observed that the d-spacing and the degree of clay dispersion changes from one location to another in the same nanocomposite.

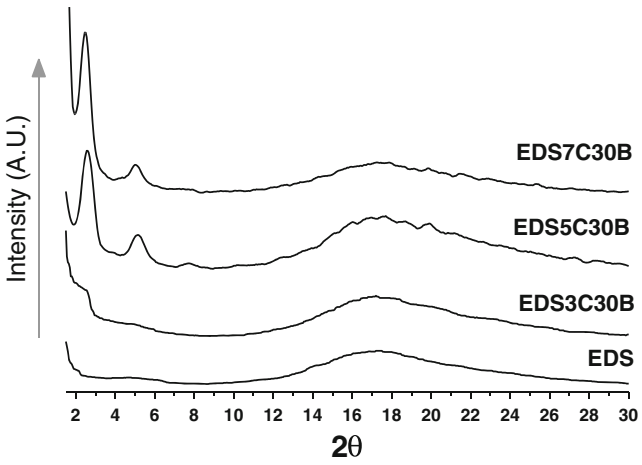

Fig. 2 X-ray diffractograms of pristine epoxy and epoxy composites with 3 %, 5 %, and 7 % of Cloisite 30B

Thermal stability

In some previous studies the thermal properties of epoxy resins [24–27] have been investigated. In nitrogen, pure epoxy resin thermally degrades through a double step process with maximum rate at 301 and 414 °C leaving a 4.1 % residue [28]. The first step of degradation involves water elimination which results in formation of C-C unsaturations [27]. Carbon-oxygen bonds in beta position to these unsaturations (allylic bonds) become the thermally weakest bonds in the epoxy network. They break down giving fragmentation of the crosslinked structure that eventually produces fragments small enough to evaporate at these temperatures. Volatilisation is, however, limited up to 350 °C because it is contrasted by rearrangements such as cyclisation that produce a relatively stable structure which breaks down in the second step of degradation. In this step extensive break down of chemical bonds of the epoxy network takes place including C-phenyl bonds of bisphenol-A, leading to almost complete volatilisation. In the air flow, Camino et al. [27] have found that the first step remains virtually unaltered while in the second degradation step, charring of the epoxy network, takes place at a higher yield (ca. 20 % at 400 °C) than in nitrogen, due to catalysis by oxygen.

In order to confirm the presence of organoclays and evaluate their influence on the thermal decomposition, the same pieces of the different sample analyzed by x-ray, were subsequently analyzed by TGA. In Fig. 4 the thermogravimetric curves, evaluated in air flow, for all the samples in the range 50–900 °C are reported. As can be seen from Fig. 4, at the initial stage of degradation (before 400 °C), the nanocomposites degrade faster than the pure matrix. On the other hand, above 400 °C nanocomposites appear to be more stable than pure epoxy matrix. Generally, it was found that the thermal stability of the polymer matrix is not sacrificed by nanocomposite formation. In some cases the clay acts as a superior insulator and mass transport barrier to the volatile products generated during decomposition, as well as by assisting in the formation of char after thermal decomposition. However, decreases in the thermal stability of polymers upon nanocomposite formation have also been reported, and various mechanisms have been put forward to explain the results [29]. It has been argued that the early stage of thermal decomposition is due to the Hoffmann elimination reaction and the clay-catalyzed degradation. At higher temperature/degree of decomposition the organoclay slows up the degradation process. Thus, all types of organoclay used show two opposing effect in thermal stability of nanocomposites: a catalytic effect on the degradation of the polymer matrix in the early stage of degradation, and a barrier effect, which should improve the thermal stability at high temperature [30]. The residue at high temperatures confirms the presence of the clay also in the case of samples that did not present any basal peak at low angle.

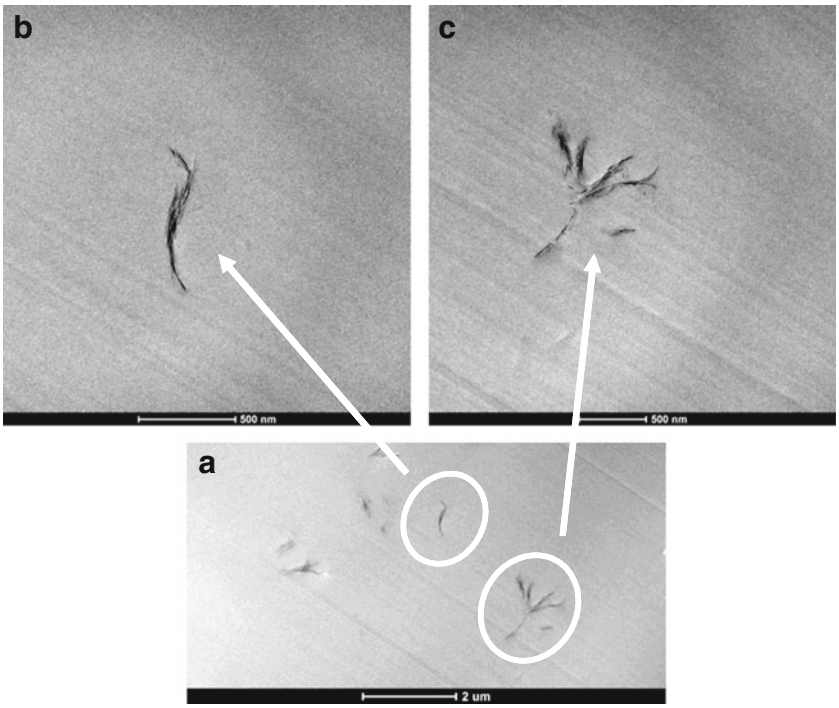

Fig. 3 High resolution transmission electron microscope images of EDS3C30B

The Table 2 reports the values of onset-degradation temperature (5 % weight-loss temperature), maximum-rate degradation temperatures (1° and 2° step) and the char yield calculated. Respect to the neat resin the values of the composite samples show a maximum rate of weight loss at a lower temperature (Table 2). Indeed the catalytic effect of clays on the degradation of the polymer matrix has been well studied by Camino and al. [27]. The catalytic activity of the clay on the polymer decomposition process is due to Bronsted and Lewis acid sites constituted by the clay lattice hydroxyl groups, which contact with the polymer matrix. This catalytic activity is large in nanocomposites. Furthermore the Hoffman decomposition of the onium modifier of clays gives protonated montmorillonite that can act as a protonic acid catalyst. The lower thermal stability of the composites, if compared to neat resin, could arise from a larger catalytic activity related to the tri-alkyl and tetra-alkyl structure of its organic modifier. This could explain why nanocomposites show lower thermal stability in the main degradation process than the epoxy resin [27].

As for the second step, the data of Table 2 show that the largest shielding effect from oxygen is obtained in the char formed from the nanocomposites EDS3C30B and EDS3N804, which show by XRD (Fig. 1) the most exfoliated structure. A lower oxidation protection is found for EDS3C93A which shows a lower degree of exfoliation as compared with EDS3C30B and EDS3N804. This is in agreement with results of Camino et al. [28].

Our data therefore agree in many respects with those obtained by Camino et al. [27], but the differences are less pronounced, because the contents of clay used for our samples (3 % by weight) are well below those used by Camino.

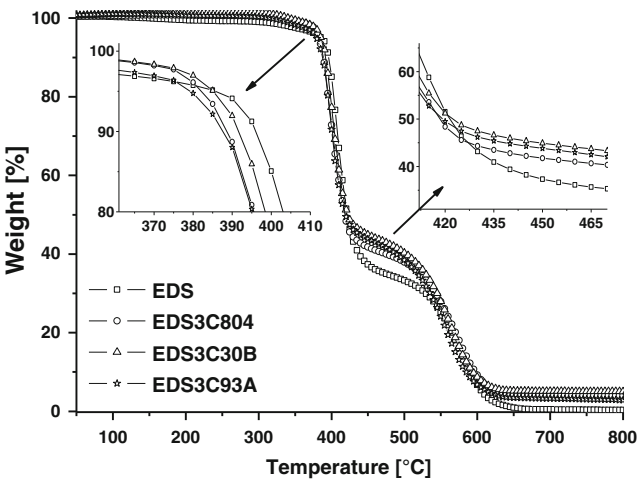

Fig. 4 TGA curves of epoxy and epoxy composites with different organoclays at 3 % of concentration

Table 2 Thermal oxidation of epoxy resin and composites

Sample	T_{max} (°C)		$T_{5wt.\%\ loss}$	Char yield $_{800°C}$
	1° Step	2° Step		(%)
EDS	400	562	386	0
EDS3C30B	393	556	385	5
EDS3N804	394	562	382	4
EDS3C93A	394	546	379	3

Kinetics of cure

In Fig. 5 the exotherms, due to the curing reactions for the pristine resin and the resin filled with the three organoclays (samples EDS3N804, EDS3C93A, and EDS3C30B), are shown. For the EDS sample, it is observed the beginning of the curing reaction at about 150 °C, with a maximum of transformation at 225.5 °C. For the three composite samples the beginning of the cure is anticipated, and the peak temperature is at lower temperature, too. The peak temperature (T_p) and the curing enthalpy for all the samples are reported in Table 3. For all the samples in the second run of heating (not shown here) no exotherm is still visible, indicating that the samples were completely cured in the first run. From Fig. 6 and Table 3 it is evident that the presence of the organoclays accelerates the curing reactions, either as beginning of the reaction or as temperature of the maximum transformation.

In other words, it can be concluded that the organoclay participate in some ways to the curing process. In Fig. 6 the percentage of cure, defined as

$$\alpha = \frac{\Delta H_T}{f * \Delta H_{tot}}$$

where ΔH_T is the enthalpy of reaction, ΔH_{tot} the total enthalpy of reaction and f is the weight fraction of the resin, is reported as a function of the temperature for the pristine and the composites with various percentages of Cloisite 30B. In Table 3 the cure enthalpy (ΔH_{tot}) and the temperature of maximum transformation for these samples are also reported.

The ammonium ions of primary and tertiary amines have been used in the past to treat layered silicate clays. In epoxy–clay systems, the ammonium ions catalyze both epoxy homopolymerization and epoxy-diamine reactions, thereby creating a disparity in the curing rates of epoxy

Table 3 Peak temperature and curing enthalpy for pristine epoxy and epoxy composites with different organoclay types and concentrations

Sample	T_p (°C)	ΔH_{tot} (J/g)
EDS	225,5	401±16
EDS3N804	220,2	352±14
EDS3C93A	216,5	423±25
EDS3C30B	221,5	335±13
EDS5C30B	219,2	325±12
EDS7C30B	218,4	322±15

inside and outside the clay galleries [31]. The curing rate increases with the acidity of the ammonium ions, e.g. ammonium ions of primary alkyl amines are more acidic than quaternary ammonium ions [32]; Probably the lower temperature of maximum transformation of EDSC93A is due to the higher acidity of the Methyl Hydrogenated Tallow Ammonium compared to the other organic modifiers. We found that the exothermic peaks of the clays/epoxy composites were smaller than that of the neat epoxy, implying that the addition of clays decreased the extent of conversion of the epoxy resins. This is possibly because the existence of the clays physically hinders the mobility of the epoxy monomers and also affects the optimized curing ratio between DGBDA and DDS

The temperature of the maximum transformation decreases on increasing the organoclay concentration. Indeed the composite with 7 % of clays shows the temperature peak 7° lower than the pristine resin. These results demonstrate and confirm that the surface modifier of the nanoclay accelerates the cure process, as previously reported [33, 34]. It was demonstrated that acidic onium ions (i.e. acidic cations) of diamines catalyze the intragallery epoxide polymerization process. The higher reactivity of the ammonium surface modifier explains why a greater proportion of nanoclay in the nanocomposite increases the epoxide conversion during the initial cure stage.

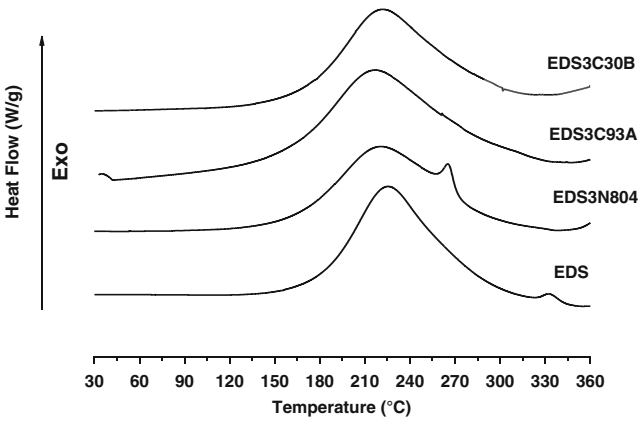

Fig. 5 Heating curves of pristine epoxy and epoxy composites with different organoclays at 3 % of concentration

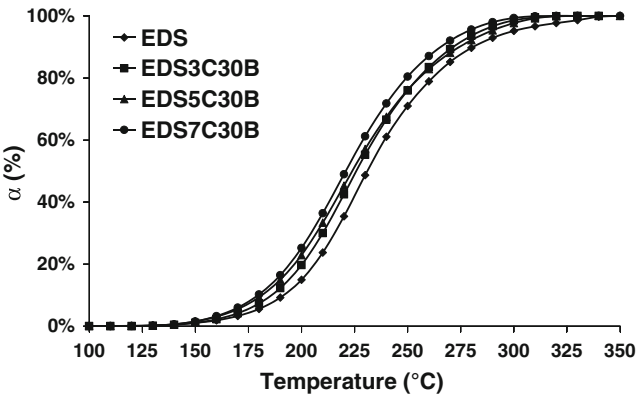

Fig. 6 Percentage of cure of pristine epoxy and epoxy composites with 3 %, 5 % and 7 % of Cloisite 30B

Density behaviour

The density of the pristine and composite samples was measured by a floating method. Experimental results were compared with theoretical values calculated using a simple mixing rule. The corresponding equations are:

$$f = \frac{{}^{w}/_{\rho_{Clay}}}{{}^{w}/_{\rho_{Clay}} + {}^{(1-w)}/_{\rho_{Epoxy}}} \quad (1)$$

$$\rho_c = \rho_{Epoxy}\left(1-f_{Clay}\right) + \rho_{Clay}\left(f_{Clay}\right) \quad (2)$$

where f is the volume fraction of organoclay, w the weight fraction of clay, ρ_{Clay} the clay density (see Table 1), ρ_{Epoxy} the matrix density, and ρ_c the composite density. From Fig. 7, it is evident that the experimental values are in all the cases lower than that predicted by the mixing rule indicating, probably, the presence of microvoids at the interphase between polymer matrix and clay lamellae. The quantity of these microvoids is higher in the case of sample EDS3C93A and it will influence the water sorption, as will be shown later.

In Fig. 8, the densities of the samples obtained with Cloisite 30B as function of the volume fraction of the organoclay content are reported. The uncertainty in the measured densities is estimated from a propagation of errors analysis. Sample density, both measured and calculated, increases with organoclay content, consistent with the fact that organoclay has a significantly higher density than epoxy. The measured densities of sample containing 5 and 7 wt% are somewhat lower than those calculated from the additive model (Eq. 2). This deviation from additivity suggests that incorporation of organoclay into epoxy increases free volume and microvoids in the sample. However, the differences in calculated and measured densities are near to the uncertainty in the measurements, implying that any change in sample free volume resulting from organoclay addition cannot be accurately determined with this method.

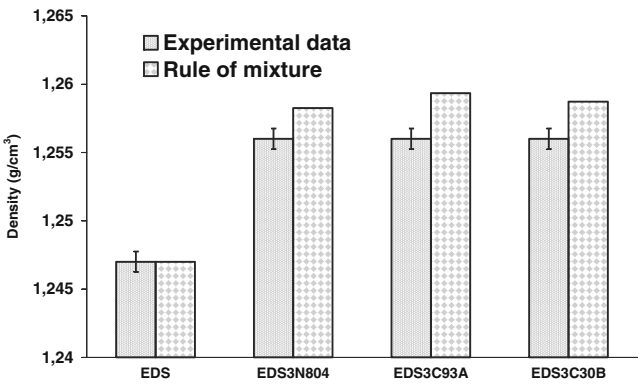

Fig. 7 Density of pristine epoxy and epoxy composites with different organoclays at 3 % of concentration

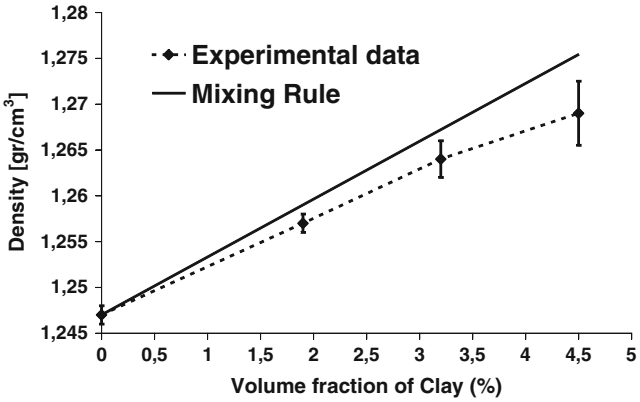

Fig. 8 Density of the composite samples as a function of volume fraction of Cloisite 30B

Water transport properties

As discussed, one of the most important physical properties to be improved for the epoxy resins is the water permeability. In addition, the use of small molecules as molecular probes can help clarify many important aspects related to the structural organization of the permeable regions in a multiphase system.

Measuring the increase of weight with time for samples exposed to the water vapour at a given partial pressure, it is possible to obtain the equilibrium value of sorbed vapour, C_{eq}. Moreover, in the case of Fickian behaviour it is possible to derive the mean diffusion coefficient from the linear part of the reduced sorption curve, reported as C_t/C_{eq} versus the square root of time, by Eq. 3

$$\frac{C_t}{C_{eq}} = \frac{4}{d}\left(\frac{Dt}{\pi}\right)^{\frac{1}{2}} \quad (3)$$

Where C_t is the penetrant concentration at time t, C_{eq} is the equilibrium value, and d (cm) is the thickness of the sample.

Diffusion depends on concentration for many polymer-solvent systems, and generally this dependence can be expressed by following empirical law of Eq. 4

$$D = D_0 \exp\left(\beta C_{eq}\right) \quad (4)$$

Where D_o is the thermodynamic zero-concentration diffusion coefficient, related to the fractional free volume and the microstructure of the system, and β is the concentration coefficient also depending on the free volume and the plasticizing effectiveness of the penetrant. The permeability of the samples to the vapours is calculated as the product of sorption and diffusion, at each vapour pressure. In contrast to many

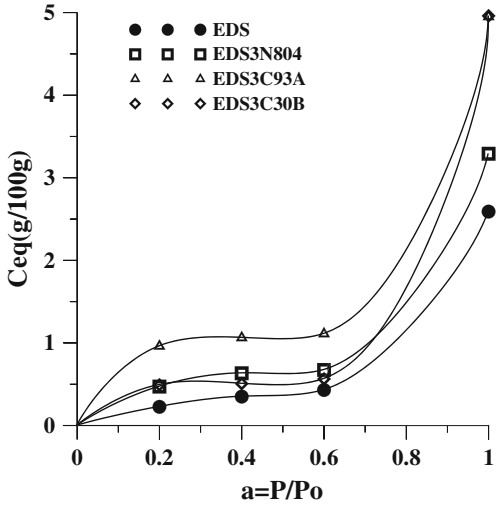

Fig. 9 The equilibrium concentration C_{eq} (g/100 g) of vapour as a function of vapour activity $a=p/p_o$ for pristine epoxy and epoxy composites with different organoclays at 3 % of concentration

papers reported in the literature where the water sorption of the material is evaluated for activity equal to 1, this work has been focused on the effect of sorption at different water activities The decrease in the maximum water uptake and diffusivity with increasing clay loading have been reported by Liu et al. [35]. However, Becker et al. [14] showed that, while the maximum water uptake decreased as a result of clay addition, the diffusivity increased. Gasem et al. [36] found no significant improvement in maximum water uptake and in diffusivity for nanoclay composites synthesized by sonication, and the nanocomposite containing 5 % of clay showed higher diffusivity and water uptake compared to neat epoxy. Kornmann et al. [37] found that the water uptake of neat epoxy and its nanoclay composites are very similar for samples tested at 23 °C; however, at 50 °C the nanocomposite water uptake is much higher than that of neat epoxy. The mixing technique used during the fabrication of nanocomposites, the effectiveness of the degassing process, the nature of the clay and the resins, in addition to the different thermal cycles of curing, appear to play a key role in the diffusion process, that explain the above-mentioned contradictory results about barrier properties of synthesized epoxy–clay nanocomposites.

In Fig. 9 the dependences of the equilibrium concentration of water vapour on the activity, $a=p/p_o$, measured at 30 °C, for pristine and composite samples are shown. The experimental data up to activity of water vapour 0.6 are jointed up to the value of equilibrium concentration measured in liquid water at 30 °C.

The sorption curves follow the Langmuir sorption behaviour, in which the sorption of the vapour molecules occurs at beginning on specific sites. When the sites are saturated a constant or a linear increase is observed. The equilibrium sorption at low activity, relative to the specific sites on which the vapour molecules are absorbed, is higher in the samples filled with organoclays. The increase is consistently strong in the case of Cloisite 93A and less evident in the other two samples. The higher content of water is due to the hydrophilic nature of the organoclays and to an increased free volume, too. As shown in Fig. 8 sample EDS3C93A has the highest free volume fraction. Moreover Cloisite 93A is the less interacting organoclay, and therefore the hydrophilic clay lamellae are less embedded in the resin and more available to the water molecules. Also the other two organoclays show a slightly higher sorption, due to the higher free volume, as also shown in Fig. 9. The connection with the equilibrium concentration at activity $a=1$ indicates that after a threshold activity the equilibrium concentration shows a more than linear increase, following a Flory-Huggins behaviour. The water molecules strongly interact with the polymeric structure, making the chains more mobile and therefore able to adsorb more and more water molecules. In this case the liquid molecules tend to form "clusters" strongly interacting with the matrix. Also in this case the sample with Cloisite 93A, with an equilibrium concentration almost double of the others, shows the worst behaviour. The values of equilibrium concentration at activities $a=0.6$ (that is almost the activity at room environmental conditions) and $a=1.0$ are reported in Table 4 for all the samples.

In Fig. 10 the diffusion coefficients, derived according to Eq. 4 as a function of the equilibrium concentration are shown. The mean parameters were extrapolated to zero vapour concentration, obtaining the D_o parameters, also reported in Table 4.

A decrease of the D_o parameter is evident for all the filled resins, even for the Cloisite 93A. The reduction of the diffusion coefficient is due to a tortuous path that the penetrant molecules have to travel and therefore is related to both the lamellar nature of the filler and the interaction with the matrix [15]. The best results are shown by Cloisite 30B, with a diffusion coefficient decreased of almost one order of

Table 4 D_0 parameters and equilibrium concentration C_{eq} *(g/100 g)* of vapour at activity $a=0.6$ and *1* for pristine epoxy and epoxy composites with different organoclays at 3 % of concentration

Sample	D_0[cm^2/sec]	Ceq(a=0.6) [g/100 g]	Ceq(a=1)[g/100 g]
EDS	$3.00*10^{-9}$	0.43	2.59
EDS3N804	$1.93*10^{-9}$	0.67	3.29
EDS3C93A	$2.43*10^{-9}$	1.11	4.95
EDS3C30B	$5.46*10^{-10}$	0.56	4.96

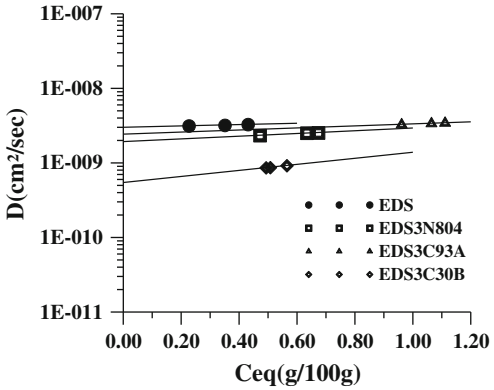

Fig. 10 The logarithm of the diffusion coefficient as a function of equilibrium concentration for pristine epoxy and epoxy composites with different organoclays at 3 % of concentration

magnitude respect to the pristine resin. The permeability, *P*, as the product *S x D*, reported in Fig. 11 is obtained if the value of the parameters at activity of water *0.6* is considered.

Since the permeability is the product of sorption and diffusion, its value depends on both these values for the composite samples. Sorption is always higher for the three composite samples and therefore the value of permeability is strictly connected to the lowering of diffusion. For this reason the value of permeability is lower only in the C30B sample, which shows a value of diffusion of an order of magnitude lower than the pristine resin. In the case of N804 and C93A, the value of diffusion is not sufficiently lower to compensate the higher sorption and therefore we observe a higher permeability for theses samples. Figure 12 shows the permeability to water of the samples, at activities *a= 0.6*, with increasing organoclay concentration. In contrast with the tortuous pat model, the permeability is reduced only in the resin with 3 % of organoclay. This is a further evidence that only the sample with 3 % of Cloisite 30B can be considered completely exfoliated.

Dynamic mechanical analysis

Dynamic mechanical analysis allows to determine the mechanical parameters (elastic modulus and stiffness) of a

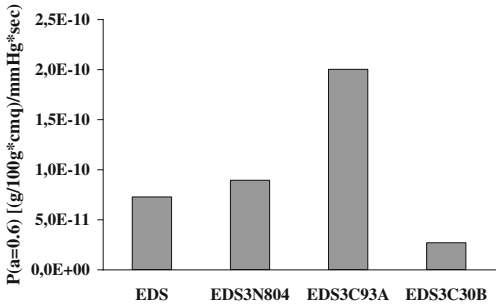

Fig. 11 Permeability at *a= 0,6* for pristine epoxy and epoxy composites with different organoclays at 3 % of concentration

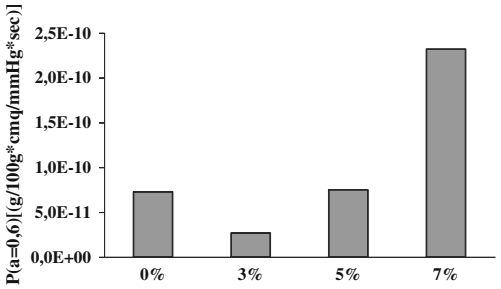

Fig. 12 Permeability at *a= 0.6* for pristine epoxy and epoxy composites with 3 %, 5 %, and 7 % of Cloisite 30B

sample subjected to a dynamic deformation in a wide range of temperature. Moreover, observing the loss factor, *tan δ,* it is possible to locate the glass transition temperature as well as secondary relaxations. Figure 13 displays the logarithm of the elastic modulus, *E'* (MPa), and the loss factor, *tan δ,* of the pristine resin and the samples with different organoclays at 3 % of concentration. For all the samples a smooth decrease of the modulus up to 80–90 °C and an almost constant value of the elastic modulus between 90 and 200 °C, followed by an evident drop due to the glass transition of the resin are evident. Indeed in the correspondence of the drop an intense peak of the *tan δ* curve indicates the glass transition temperature of the resin. The

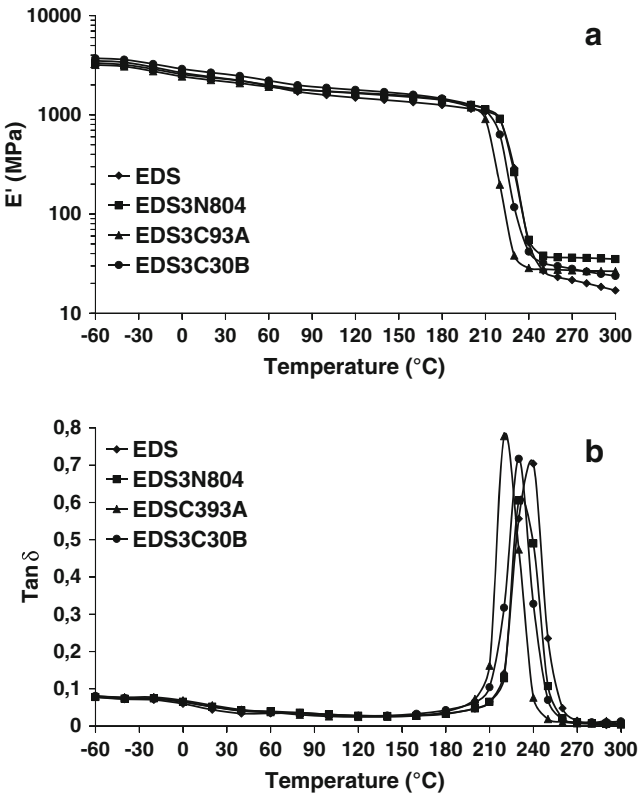

Fig. 13 Behaviour of the elastic modulus (**a**) and the loss factor (**b**) as a function of temperature, of pristine epoxy and epoxy composites with different organoclays at 3 % of concentration

numerical values of the moduli at some selected temperatures and the glass transition temperatures are collected in Table 5. The composite samples show a qualitative behaviour of the elastic modulus very similar to the pristine resin. However, only the sample with the 3 % of Cloisite 30B shows an elastic modulus higher than that of the pristine resin in all the investigated temperature range. All the other nanocomposites samples show higher elastic modulus only at high temperatures, when materials become soft. In this range, probably, the reinforcement effect of the organoclay particles becomes more prominent with respect to the polymer crosslink restriction.

However, shift of tan δ to lower temperatures is observed in all the analyzed samples. Some authors considered this behaviour as indicative of the glass transition suppression by the presence of the organoclay [47]. Fornes and Paul [38] suggest that the shift of tan δ is due to the larger storage modulus value in the glass transition region compared to the relatively constant loss modulus.

A lower Tg with higher clay content was also reported by many other investigators [39–43]. Since the clay particles have extremely high specific surface area, the good dispersion even at low clay contents provides an enormous amount of interfacial area. The interaction of the polymer chains with the surface of the particles can drastically alter the chain kinetics in the regions surrounding them and lead to a lower cross-link density. Kornmann et al. [42] suggested that Tg could be lowered due to thermal degradation of compatibilizing agents at high temperature. Another possible reason for the decrease in Tg could be the formation of an interphase between the silicate layers [43, 44]. An inter-phase has been defined as the matrix material close to the clay surface, whose properties are different from those of the bulk material. It can be formed due to plasticization of epoxy by surfactant chains as suggested by Chen et al. [43]. The higher the clay content and the d-spacing, the higher the volume fraction of interphase material. Therefore, excluding curing temperature, curing speed and degree of cross-linking as suggested elsewhere [39, 41, 45], the other important factors that can affect Tg are the surface modification treatment, level of particle dispersion and the spacing between particles. In the present study the decrease of the glass transition temperature for the various clay deployed, to be attributable to the different thermal degradation of compatibilizing agents at high temperatures, as suggested by Kornmann et al. [42].

Figure 14 shows the dynamic mechanical analysis for the samples with increasing organoclay concentration. Also in this case, the values at some selected temperatures are reported in Table 5.

In a previous study [23] the Cloisite 30B/epoxy nanocomposite were produced, and, as in our case, an increase of the % of Cloisite 30B determined a decrease in Tg due to a lower cross-link density. This is in agreement with the data relating to the lowest enthalpy of reaction, recorded for composites. The modulus of the sample with 5 % and 7 % of organoclay is still higher than the pristine resin, although slightly lower than that with 3 %. The main conclusion derived from dynamic mechanical studies is that the storage modulus increases upon dispersion of a layered silicate in a polymer. This increase is generally larger above the glass transition temperature, and it is probably due to the creation of a three-dimensional network of interconnected long silicate layers [38, 46]. In other words the sample to 3 % has a storage modulus highest because it shows an exfoliated structure, presenting an exposed surface of the clay larger than an intercalated structure obtained in the case of 5 and 7 %; this causes a higher interaction with the matrix and a consequent greater reinforcement

Effects of moisture on thermo-mechanical properties

In order to verify the effect of the water molecules on the mechanical properties of the composites, selected samples were immersed in distilled water at 30 °C for 45 day. This time was sufficient for reach the equilibrium water content in all samples. In Figs. 15 and 16 the elastic modulus and the loss factor (tan δ) of the pristine epoxy and the EDS3C30B sample before and after the water immersion are reported. The elastic modulus, for both samples, shows a decrease in all the temperature range. However, at lower temperatures, the changes observed for EDS (less than 10 %) are lower with respect to that observed for EDS3C30B sample (higher than 15 %). It is probably due the higher content of water in the sample (Fig. 9) that plasticize the polymeric matrix. The tan δ curves show a double peak in both samples. In

Table 5 Glass transition temperature and storage modulus of pristine epoxy and epoxy composites with different organoclays at selected temperatures

Sample	Tg (°C)	−10 (°C)	30 (°C)	90 (°C)	120 (°C)	260 (°C)	280 (°C)
EDS	236	2820	2314	1636	1486	23	20
EDS3N804	234	2703	2288	1763	1647	36	36
EDS3C93A	223	2569	2157	1757	1669	27	26
EDS3C30B	230	3062	2559	1922	1781	29	26
EDS5C30B	227	2918	2457	1833	1710	35	32
EDS7C30B	226	2909	2251	1621	1424	46	84

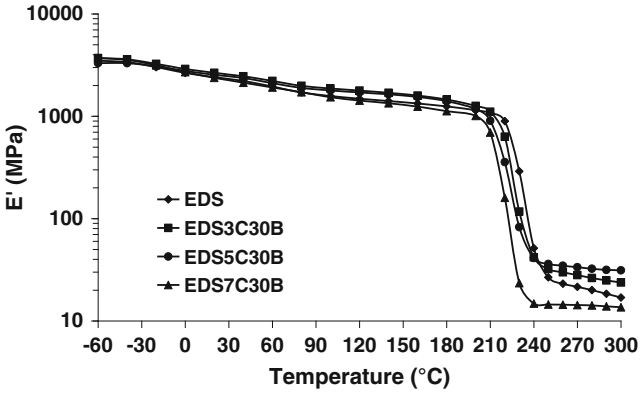

Fig. 14 Behaviour of the elastic modulus as a function of temperature for pristine epoxy and epoxy composites with 3 %, 5 % and 7 % of Cloisite 30B

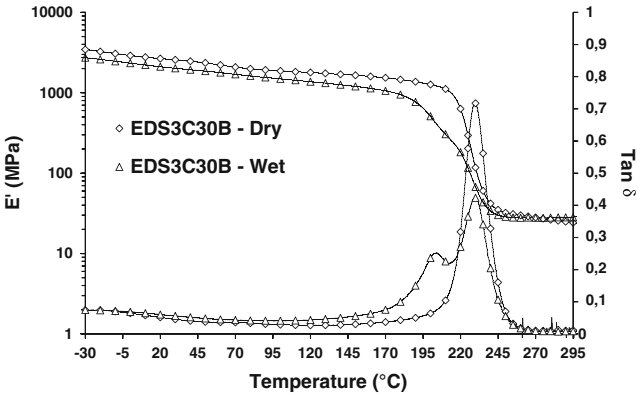

Fig. 16 Elastic moduli and loss factor (tan δ) of dry and wet EDS3C30B samples

particular, the tan δ height was diminished in the region of the glass transition temperature of the dry material and it is followed by a new peak of tan δ in the temperatures below the Tg. It can be explained in terms of free volume and epoxy-water interactions [12, 26, 29, 47, 48]. The rupture of the hydrogen bonding between polymer chains by water molecules would produce an increment of the chain mobility during the glass transition region and therefore a higher free volume of the material.

The large variation in elastic modulus of the composites samples, probably, is due to the presence of water molecules in the interface between the polymer matrix and the clay sheets that modify the constraints of the polymer chain mobility near the reinforcements.

In previous studies, the effect of the layered silicate on the thermal relaxation of the dry specimens has been the subject of discussions and it was found that both, the α- and β-relaxation peak temperature are constantly decreased with increasing organoclay concentration, possibly to a number of reason, such as changes in reaction chemistry, lower crosslink density or a plasticizing effect of the clay compatibilizer or entrapped resin or hardener monomers. In particular, this is seen in other

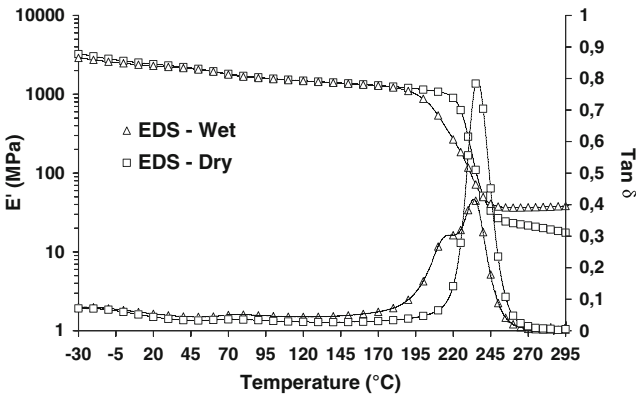

Fig. 15 Elastic moduli and loss factor (tan δ) of dry and wet epoxy samples

systems with rigid amines and high functionality epoxy resins [49].

Becker et al. [14] have obtained a single peak of tanδ for a DGEBA epoxy resin, which moves to the lowest temperature after absorption of water, while a double peak was obtained for resins with functionalities greater than 2. The difference in results with our samples is probably due to a number of reasons. We have a fraction of resin that remains unchanged, while Becker et al. obtained, for the base resin of DGEBA, a complete plasticization. Such behavior is due to the different chemical nature of the hardener and the ratio DGEBA / hardener. In fact they use an excess of epoxy group which causes a greater percentage of homopolymerization, which change the affinity of the resin with the water due to hydrogen bonds with the ether oxygen.

Conclusions

The thermo-mechanical properties and the moisture barrier characteristics were studied for epoxy nanocomposites containing three different organoclays. The X-ray analysis indicates that, depending on the organoclay type, partially exfoliated and partially intercalated composites have been obtained. The dynamic curing of the resin in the presence of the organoclays indicates a kinetic effect on the cross-linking reaction. The densities of the composite samples are systematically lower than that predicted by a simple mixing rule. This suggests that incorporation of organoclay into epoxy increases free volume and micro-voids in the sample.

In all samples, the sorption of water results slightly higher than the pristine resin, due to the hydrophilic nature of the clays. In contrast, the diffusion coefficient is significantly lower for all the composite samples. However, since the permeability is the product of sorption and diffusion, the value of this parameter is lower than the pristine resin only in the case of the sample with a prevalently exfoliated structure, for

which, in spite of a higher sorption, the diffusion is lower of an order of magnitude. The elastic modulus of the composites samples results higher than that of the pristine epoxy matrix, especially in the region around the glass transition. The presence of organoclay in epoxy matrix decreases the glass transition temperature, whether the nanocomposites were in a dry or wet condition. The T_g for both the nanocomposite and neat epoxy display a strong reduction with increasing the moisture content.

Acknowledgments "The activities were performed in the frame of the project "IMPRESA" (DM 60704) granted to IMAST S.c.a.r.l. and funded by the M.I.U.R."

References

1. Klaus F, Stoyko F, Zhong Z (2010) Polymer composites: From nano- to macro scale. Springer, New York
2. De Nograro FF, Guerrero P, Corcuera MA, Mondragon I (1995) Effects of chemical structure of hardener on curing evolution and on the dynamic mechanical behavior of epoxy resins. J Appl Pol Sci 56:177–192
3. Vieth WR (1991) Diffusion in and through polymers: principles and applications. Hanser, New York
4. Jelinsky LW, Dumais JJ, Colli AL, Ellis TS, Karasz FE (1985) Nature of the water-epoxy interaction. Macromolecules 18:1091–1095
5. Woo M, Piggott M (1987) Water absorption of resins and composites II: diffusion in carbon and glass reinforced epoxies. J Comp Tech Res 9:162–166
6. Apicella A, Nicolais L, Mikols WJ, Seferis JC (1984) Interrelation between processing structure and properties of polymeric materials. Seferis JC, Theocaris PS Elsevier, Amsterdam, p 189
7. Apicella A, Nicolais L, Cataldis C (1985) Characterization of the morphological fine-structure of commercial thermosetting resins through hygrothermal experiments. Adv Polym Sci 66:189–207
8. Moy P, Karasz FE (1980) Epoxy-water interaction. Polym Eng Sci 20:315–319
9. Glaskova T, Aniskevich A (2009) Moisture absorption by epoxy/montmorillonite nanocomposite. Compos Sci Technol 69:2711–2715
10. Pethrick RA, Hollins EA, Mc Ewan I, Pollock EA, Hayward D (1996) Effect of cure temperature on the structure and water absorption of epoxy/amine thermosets. Polym Int 39:275–288
11. Barral L, Cano J, Lopez J, Lopez-Bueno I, Nogueira P, Abad MJ, Torres A, Ramirez C (2000) Mechanical behavior of tetrafunctional/phenol novolac epoxy mixtures cured with a diamine. J Appl Polym Sci 77:2305–2313
12. Nogueira P, Ramirez C, Torres A, Abad MJ, Cano J, Lopez J, Lopez-Bueno I, Barral L (2001) Effect of water sorption on the structure and mechanical properties of an epoxy resin system. J Appl Polym Sci 80:71–80
13. Wang Z, Massam J, Pinnavaia TJ (2000) Epoxy-clay nanocomposites. In: Pinnavaia TJ, Beall GW (eds) Polymer clay nanocomposites. Wiley Chichester, p 127–148
14. Becker O, Varley RJ, Simon GP (2004) Thermal stability and water uptake of high performance epoxy layered silicate nanocomposites. Eur Polymer J 40:187–195
15. Sorrentino A, Tortora M, Vittoria V (2006) Diffusion behavior in polymer-clay nanocomposites. J Polymer Sci, Part B: Polymer Phys 44:265–274
16. Ratna D, Manoj NR, Varley R, Singh Raman RK, Simon GP (2003) Clay reinforced epoxy nanocomposites. Polym Int 52:1403–1407
17. Guadagno L, De Vivo B, Di Bartolomeo A, Lamberti P, Sorrentino A, Tucci V, Vertuccio L, Vittoria V (2011) Effect of functionalization on the thermo-mechanical and electrical behavior of multi-wall carbon nanotube/epoxy composites. Carbon 49:1919–1930
18. Guadagno L, Naddeo C, Vittoria V, Sorrentino A, Vertuccio L, Raimondo M, Tucci V, Russo S (2010) Cure behavior and physical properties of epoxy resin-filled with multiwalled Carbon nanotubes. J Nanosci Nanotechnol 10:2686–2693
19. Guadagno L, Vertuccio L, Sorrentino A, Raimondo M, Naddeo C, Vittoria V, Iannuzzo G, Russo S (2009) Mechanical and barrier properties of epoxy resin filled with multi-walled carbon nanotubes. Carbon 47:2419–2430
20. Vertuccio L, Gorrasi G, Sorrentino A, Vittoria V (2009) Nano clay reinforced PCL/starch blends obtained by high energy ball milling. Carbohydr Polym 75:172–179
21. Neitzert HC, Sorrentino A, Vertuccio L (2010) Epoxy/MWCNT Composite Based Temperature Sensor with Linear Characteristics. In: Malcovati P, Baschirotto A, d'Amico A, Natale CD (eds) Sensors and Microsystems: AISEM 2009 Proceedings, vol 54. Berlin
22. Sorrentino A, Gorrasi G, Tortora M, Vittoria V (2006) Barrier properties of polymer/clay nanocomposites. In: Yiu-Wing Mai, Zhong-Zhen Yu (eds) Polymer Nanocomposites, Chapter 11. Cambridge, p 273–292
23. Yasmin A, Luo JJ, Abot JL, Daniel IM (2006) Mechanical and thermal behavior of clay/epoxy nanocomposites. Compos Sci Technol 66:2415–2422
24. Levchik SV, Camino G, Luda MP, Costa L, Muller G, Costes B et al (1996) Epoxy resins cured with aminophenylmethylphosphine oxide. 1. Combustion performance. Polym Adv Technol 7:823–830
25. Levchik SV, Camino G, Luda MP, Costa L, Costes B, Henry Y et al (1995) Mechanistic study of thermal behavior and combustion performance of epoxy resins. I. Homopolymerized TGDDM. Polym Adv Technol 6:53–62
26. Levchik SV, Camino G, Costa L, Luda MP (1996) Mechanistic study of thermal behavior and combustion performance of carbon fiber-epoxy resin composites fire retarded with a phosphorus-based curing system. Polym Degrad Stab 54:317–322
27. Camino G, Tartaglione G, Frache A, Manferti C, Costa G (2005) Thermal and combustion behavior of layered silicate-epoxy nanocomposites. Polym Degrad Stab 90:354–362
28. Camino G, Tartaglione G, Frache A, Manferti C, Finocchiaro P, Falqui L. Fire and Polymers IV: Materials and concepts for Hazard prevention. In: Wilkie CA, Nelson GL (eds) ACS Symposium Series, Oxford University Press
29. Ray SS, Okamoto M (2003) Polymer–layered silicate nanocomposite: a review from preparation to processing. Prog Polym Sci 28:1539–1641
30. Zhao C, Qin H, Gong F, Feng M, Zhang S, Yang M (2005) Mechanical, thermal and flammability properties of polyethylene/clay nanocomposites. Polym Degrad Stab 87:183–189
31. Park J, Jana SC (2004) Adverse effects of thermal dissociation of alkyl ammonium ions on nanoclay exfoliation in epoxy-clay systems. Polymer 45:7673–7679
32. Lan T, Kaviratna PD, Pinnavaia TJ (1995) Mechanism of clay tactoid exfoliation in epoxy-clay nanocomposites. Chem Mater 7:2144–2150
33. Triantafillidis CS, Le Baron PC, Pinnavaia TJ (2002) Thermoset epoxy-clay nanocomposites: the dual role of α, ω-diamines as clay surface modifiers and polymer curing agents. J Solid State Chem 167:354–362
34. Carrasco F, Pagès P (2008) Thermal degradation and stability of epoxy nanocomposites: influence of montmorillonite content and cure temperature. Polym Degrad Stab 93:1000–1007

35. Liu W, Hoa SV, Pugh M (2005) Fracture toughness and water uptake of high-performance epoxy/nanoclay nanocomposites. Compos Sci Technol 65:2364–2373
36. Gasem ZM, Merah N, Adinoyi MJ, Khan Z (2012) The effects of clay content and sonication time on water uptake in epoxy-organoclay nanocomposites. Adv Mater Res 445:509–513
37. Kornmann X, Rees M, Thomann Y, Necola A, Barbezat M, Thomann R (2005) Epoxy-layered silicate nanocomposites as matrix in glass fibre-reinforced composites. Compos Sci Technol 65:2259–2268
38. Fornes TD, Yoon PJ, Hunter DL, Keskkula H, Paul DR (2002) Effect of organoclay structure on nylon 6 nanocomposite morphology and properties. Polymer 43:5915–5933
39. Zilg C, Mulhaupt R, Finter J (1999) Morphology and toughness/stiffness balance of nanocomposites based upon anhydride-cured epoxy resins and layered silicates. Macromol Chem Phys 200:661–670
40. Lee A, Lichtenhan JD (1996) Thermal and viscoelastic property of epoxy clay and hybrid inorganic–organic epoxy nanocomposites. J App Poly Sci (73):1993–2001
41. Becker O, Varley R, Simon G (2002) Morphology, thermal relaxation and mechanical properties of layered silicate nanocomposites based upon high-functionality epoxy resins. Polymer (43):4365–4373
42. Kornmann X, Berglund LA, Lindberg H (2000) Stiffness improvements and molecular mobility in epoxy-clay nanocomposites. Mat Res Soc Symp 628:CC11.8
43. Chen J-S, Poliks MD, Ober CK, Zhang Y, Wiesner U, Giannelis E (2002) Study of the interlayer expansion mechanism and thermal-mechanical properties of surface-initiated epoxy nanocomposites. Polymer 43:4895–4904
44. Vaia RA, Giannelis EP(2001) Polymer nanocomposites: status and opportunities. MRS Bull, May
45. Lan T, Pinnavaia TJ (1994) Clay-reinforced epoxy nanocomposites. Chem Mater (6):2216–2219
46. Fornes TD, Paul DR (2003) Modeling properties of nylon 6/clay nanocomposites using composite theories. Polymer 44:4993–5013
47. Vanlandingham MR, Edduljee RF, Gillespie JW Jr (1999) Moisture diffusion in epoxy systems. J Appl Polym Sci 71:787–798
48. Lee MC, Peppas NA (1993) Water transport in graphite/epoxy composites. J Appl Polym Sci 47:1349–1359
49. Kornmann X, Thomann R, Mulhaupt R, Finter J, Berglund L A (2002) High performance epoxy layered silicate nanocomposites. Polym Eng Sci (42):1815–1826